The Effect of Using Epoxy As a Substitute For Hydroxyl-Terminated Polybutadiene (HTPB) on Manufacturing Solid Propellants

Maryono maryono^{1⊠}, Muhammad.Ali², Lazuardi Lazuardi³

^{1,2}Army Polytechnic Of Malang, Indonesia ³PGRI Wiranegara University Pasuruan, Indonesia

maryono250375@gmail.com, muhammad.ali@gmail.com, Atingthok99@gmail.com

Article Information

Manuscript Received 2024-07-05 Manuscript Revised 2024-10-18 Manuscript Accepted 2024-10-20 Manuscript Online 2024-10-20

ABSTRACT

The solid propellant consists of ammonium perchlorate (AP)/Hydroxyl- Terminated Polybutadiene (HTPB) composite material. In this research, innovation was carried out using epoxy as a substitute for HTPB. The analysis carried out in this research includes analysis of fuel propagation speed, combustion temperature, exit pressure, gas speed, and thrust force. Based on the results of research that has been carried out, increasing the addition of epoxy results in a decrease in combustion speed, combustion temperature, exit pressure, and combustion gas speed so that the resulting thrust force decreases. The most optimum composition in this research was composition A using 46% Ammonium Perchlorate, 36% Aluminum, and 18% Epoxy. The resulting thrust force on composition A is 750.5771 N. The difference in the thrust force results between HTPB and composition A is 1.8731 N. This proves that epoxy can be used as a substitute for HTPB.

Keywords: Ammonium perklorat, Composite, Epoxy, Hydroxyl-Terminated Polybutadiene (HTPB), Thrust Force.

1. INTRODUCTION

The use of solid propellants is increasing for various military systems in developing rocket artillery propulsion technology and missile technology [1], [2]. Combustion rate and pressure index are two important characteristic parameters for evaluating the combustion performance of solid propellants [3], [4]. Solid propellants have advantages including long-term shelf life, high solid propellant combustion rates of more than 50 mm/sec, minimum condensation, and high-speed combustion propulsion systems, high specific impulse, and low pressure index [5], [6], [7]. The solid propellant consists of (AP)/Hydroxyl-Terminated ammonium perchlorate Polybutadiene (HTPB) composite material [8], [9].

AP is the most commonly used oxidant in solid propellants. The oxygen content of AP is very high so it has good thermal and chemical stability, and gas decomposition. The thermal properties and combustion characteristics of AP have a major influence on the combustion and safety of solid propellants [10], [11]. HTPB functions as a polymer binder. HTBP is widely applied to various solid missiles. The disadvantage of using HTBP in solid propellants is that it does not have a strong interfacial bond with the polar filler, so it experiences dewetting during deformation. Dewetting will have an adverse impact on the mechanical properties, combustion performance, and storage stability of the propellant [12], [13]. So innovation is needed to

replace HTPB as a polymer binder in the manufacture of solid propellants.

Epoxy resin is an adhesive material for binding polymers. Resin-based composite materials play an important role as a binder [14], [15], [16]. Epoxy resin has excellent bond strength, stable chemical structure, high mechanical strength, excellent adhesion, high content of C and H elements, and has flammable properties [17], [18].

Based on the background description that has been explained, this research carried out research on the use of epoxy as an alternative material (binder) to replace HTPB in composite propellants. This research will look at the effect of epoxy on burn speed, specific heat, propellant gas pressure, gas velocity, gas flow rate and propellant thrust force.

2. RESEARCH SIGNIFICANCE

This research is important because it examines the potential of epoxy as an alternative to Hydroxyl-Terminated Polybutadiene (HTPB) in making solid propellants. HTPB has long been used as the main binder in propellants because it is flexible, stable, and able to bind other components well. However, HTPB has several limitations, especially in terms of production processes and costs. By exploring the use of epoxy, this research aims to find alternative materials that are not only more economical but also have characteristics that can improve propellant

performance, such as strength, thermal stability and combustion process control. The results of this research are expected to contribute to the development of more efficient propellants and perhaps also expand propellant applications in various industrial sectors.

3. RESEARCH METHODS

The materials used in this research were Ammonium Perchlorate (NH₄ClO₄), Aluminum (Al), Epoxy A and B, PVC pipe. The tools used in this research used a stirrer, propellant printer, thrust test tool, battery, chamber and nozzle, nickel wire or igniter, and a digital camera. Making composite propellant using epoxy as a binder is carried out in stages as shown in Figure 1.

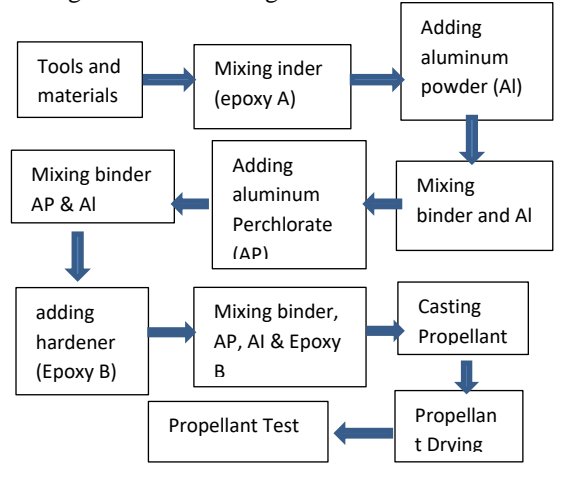


Figure 1. Steps for Making Propellant

Figure 1 shows the steps for making Propellant. The first step is to prepare the tools and materials used. Weighing Ammonium Perchlorate (NH4ClO4), Aluminum (Al), and Epoxy according to the specified material composition. The composition of the materials used is shown in Table 1.

The second step is to make propellant by putting the Epoxy A (Resin) material into a mixing container, then stirring the Epoxy A (Resin) material until evenly distributed. Add Aluminum Powder to the Epoxy A (Resin) mixture. Stir the mixture between Epoxy A (Resin) and Aluminum Powder until smooth and completely homogeneous. Ammonium Perchlorate (AP) to the mixture of Epoxy A (Resin) and Aluminum Powder. Stir the mixture of Epoxy A (Resin), Ammonium Perchlorate (AP) and Aluminum Powder until smooth and completely homogeneous. Add Epoxy B (Hardener) to the mixture of Aluminum Powder, Epoxy A (Resin) and Ammonium Perchlorate (AP). Stir the mixture of Epoxy B (Hardener), Epoxy A (Resin), Ammonium Perchlorate (AP) and Aluminum Powder until smooth and completely homogeneous. After mixing the composition completely homogeneous, the next step is to pour the propellant mixture into the container/mold. After the mixture is put into the container/mold, the propellant mixture is then dried by drying it in the sun or heating it in the oven until the propellant mixture hardens.

Table 1. Propellant Composition

	Total mass	Percentage				
Composition	Push stuffing (grams)	Ammonium Perchlorate (gram)	Alumunium (gram)	Epoxy (gram)		
A	50	23	18	9		
В	50	24	16	10		
C	50	25	14	11		
D	50	26	12	12		
Е	50	27	10	13		
F	50	28	8	14		
G	50	29	6	15		
Н	50	30	4	16		
I	50	31	2	17		

Propellant Rapid Combustion Testing Procedure

Procedure/steps for rapid combustion testing using the Strand Burning Test method by measuring the height, diameter and mass of the propellant to be tested. Prepare the propellant in the testing equipment container in a standing position. Prepare a camera, stopwatch and stationery to record the time of test results. Burn the tip of the propellant using an igniter, measure the time from the start of the combustion to the end of the propellant using a stopwatch. Record the measurement results into the data collection table.

Thrust Force Testing Procedure

The procedure/steps for testing the thrust force are to insert the propellant prepared for the thrust test into the chamber, then install the nozzle on the propellant and the nozzle is then installed on the thrust force test equipment and prepare a digital camera to record the magnitude of the change in thrust force. Insert the igniter that has been connected to the cable into the chamber through the nozzle hole, check the igniter cable using an ammeter to determine the current connection through the cable. After the check is complete, turn on the camera in the record position, then look for a safe position to start testing. After all the test instruments are ready and the position is completely safe, connect the igniter cable to the current (battery), until combustion occurs in the chamber, observe the combustion process that occurs. After the test is complete, then turn off the camera and remove the chamber from the test equipment holder for cleaning and preparation for the next thrust test.

Data processing

Data processing was obtained from the results of video analysis of the thrust force test recordings using Nerro 2016 software, to determine changes in thrust force with each change in time. Calculation of Propellant Burning Rate (r) uses the formula as shown in Equation 1.

$$r = \frac{L}{t_h} \tag{1}$$

where L is the propellant length and to is the combustion time. Calculation of the specific heat ratio value (k) can use the formula as shown in Equation 2.

$$k = \frac{c_p}{c_n} \tag{2}$$

where Cp is the heat capacity at constant pressure and Cv is the heat capacity at constant volume. Calculation of the hot area of the exit nozzle (A_{exit}) using the formula in equation 3.

$$A_{exit} = \frac{1}{4} \eth D^2 \tag{3}$$

where D is the nozzle diameter. Calculation of the crosssectional area of the throat nozzle (Athroat) using the formula in Equation 4.

$$A_{throat} = \frac{1}{4} \eth D^2 \tag{4}$$

Calculation of the ratio of exit and throat areas (A*) can use the formula in Equation 5.

$$A^* = \frac{A_e}{A_{th}} \tag{5}$$

The calculation of the ratio of exit and throat areas using the Mach number can be calculated using the formula in

$$\frac{A_e}{A_{th}} = \frac{1}{Ma} \left[\frac{1 + \frac{k-1}{2} M a^2}{1 + \frac{k-1}{2}} \right]^{\frac{K+1}{2(K-1)}}$$
(6)

The Mach number (Ma) used is 0.2. Calculation of propellant combustion temperature (To) can use Equation

$$T_o = T_e \left[1 + \frac{1}{2} (k - 1) M a^2 \right] \tag{7}$$

Where Te is the exit temperature. Calculation of the pressure of the combustion gas in the chamber can be calculated using Equation 8.

$$P_c = \left[\frac{\frac{k-1}{k}}{\sqrt{\left(Ma^2 \frac{k-1}{2}\right) + 1}}\right] P_{atm} \tag{8}$$

The atmospheric pressure (Patm) used is 1 bar. Calculation of pressure at the throat can be calculated using Equation 9.

$$P_{th} = P_c \left[1 + \frac{k-1}{2} \right]^{-\frac{k}{k-1}} \tag{9}$$

Calculation of the gas flow velocity coming out of the nozzle (Ve) can be calculated using Equation 10.

$$V_e = \sqrt{\frac{2kRT_o}{k-1} \left[1 - \left(\frac{P_c}{P_{th}} \right)^{\frac{k-1}{k}} \right]}$$
 (10)

Calculation of the mass flow rate of propellant combustion gas (m) can be calculated using Equation 11.

$$\dot{m} = A_{th} P_{th} k \frac{\sqrt{[2/(k+1)]^{(k+1)(k-1)}}}{\sqrt{k}} \tag{11}$$
 Calculation of rocket thrust can be calculated using

equation 12.

 $F = \dot{m} V_e + (P_e - P_{atm}) A_e$ (12)

RESULT and DISCUSSION **Propellant Burning Rate (r)**

The results of testing the burning rate of APCP propellant with HTPB as a binder, it is shown in Table 2. The results of the graph of burning rate against burning time with variations in propellant mass are shown in Figure 2.

Table 2. Fast Propellant Combustion Calculation Result.

C	L	tb	r
Composition	cm	det	cm/det
APCP HTPB	10	39,75	0,252
A	10	68,75	0,145
В	10	73,25	0,137
С	10	77	0,130
D	10	79,5	0,126
Е	10	80,75	0,124
F	10	84,25	0,119
G	10	87,75	0,114
Н	10	89	0,112
I	10	93,5	0,107

Specific Heat Calculation Results (k)

The results of the calculation of the specific heat ratio value are shown in Tables 3 and 4.

Table 3. Table of Gases At Low Pressures

No	T (°K)	t (°C)	Cp (J/kg. °K)	Cv (J/kg. °K)	k = Cp/Cv
18	550	276,85	1039,4	752,4	1,3814
19	600	326,85	1050,7	763,6	1,3760

Material Composition	Combustion Temperature °C	Specific Heat Ratio (k)	Combustion Temperature (°C)	Combustion Temperature (°K)	T0 (°K)
НТРВ	278	1,3812758	278	551,15	1591,789
A	248	1,3845735	248	521,15	1518,013
В	241	1,3853435	241	514,15	1500,655
С	233	1,3862235	233	506,15	1480,634
D	227	1,3868835	227	500,15	1465,583
Е	223	1,3872619	223	496,15	1455,345
F	217	1,3878259	217	490,15	1439,786
G	211	1,3883899	211	484,15	1424,299
Н	209	1,3885779	209	482,15	1419,105
I	201	1,3896119	201	474,15	1399,297

The test was carried out using a propellant mass of 50 grams on a propellant composition that used HTPB as a binder. It was found that the combustion temperature at the exit nozzle was 278°C. The graphical results of the ratio of

specific heat to propellant combustion temperature with variations in composition are shown in Figure 3. The Combustion of APCP propellant with HTPB as a binder with a mass of 50 grams, and using a nozzle with a throat diameter of 8 mm, obtained an exit temperature of 278 °C or 551.15 °K.

Calculation Results of Nozzle Exit Gas Velocity (Ve)

The gas flow velocity out of the nozzle using the APCP composition with HTPB as a binder. The mass flow rate of

the APCP composition with HTPB as a binder and a throath diameter at the nozzle of 8 mm resulting from propellant combustion passing through the nozzle. The rocket thrust force is APCP composition with HTPB as a binder and uses a nozzle with a throat diameter of 8 mm and an exit diameter of 18 mm.

Table 5.	Nozzle	Exit	Gas '	Velocity	(Ve).	Gas	Mass	Flow Rate

Nozzle Exit				(0), 000	Gas Mass	
Material Composition	Gas Speed (Ve)	P _c (Bar)	P _{th} (Bar)	P _e (Bar)	Flow Rate (m)	Thrust Style (F)
	(m/s)	46,6344	24,7841	26,67623	(kg/s)	(N)
HTPB	794,3719	46,9524	24,9267	26,57205	0,125555861	752,4502
A	776,6703	47,0330	24,9634	26,55023	0,129417401	750,5771
В	772,4317	47,1151	24,9999	26,52023	0,130380090	750,2172
С	767,5053	47,1802	25,0291	26,49924	0,131479578	749,6558
D	765,5043	47,2244	25,0496	26,49041	0,132329383	749,5093
Е	761,2063	47,2733	25,0710	26,46907	0,131506507	749,1617
F	757,2817	47,3364	25,0999	26,45438	0,133764127	748,7404
G	753,3507	47,3551	25,1083	26,44835	0,134663559	748,5185
Н	752,0268	47,4578	25,1544	26,41487	0,134961245	748,4108
I	747,0378				0,136197911	747,8097

Solid propellant composites are high-energy materials that have the ability to produce high-temperature gas products through self-combustion. The total energy produced by the combustion of the propellant mass under controlled conditions is directly related to the thrust available for propulsion. This propellant is safe to use and provides high performance compared to other types of solid propellants [19], [20].

Oxidizers are major components in propellant formulations and hence their decomposition plays an important role in the overall propellant combustion process. The interaction initially occurs at the interface of the AP and the fuel binder and as a result, the primary flame appears. This causes heat release through convective and conductive mechanisms that facilitate temperature rise to aid fuel pyrolysis. The decomposed product vapor appears in the form of an oxidizer-rich diffusion flame. The rate of diffusion of fuel vapor into oxidizing decomposition products determines the flame morphology and temperature. The combustion reaction occurs in a gas mixture and is thought to occur very quickly compared to the diffusion rate [21], [22].

Thermal decomposition mechanism of AP workhorse oxidizers commonly used in solid propellant composites. AP molecules contain onium salts, complex compounds formed by the transfer of protons from the acid in question to a base. Embedded onium salt protons can be transferred from cations to anions via decomposition/dissociation which produces initial acid and base molecules. Equilibrium proton transfer causes disassociative sublimation of AP and the formation of ammonia and perchloric acid. This can occur in condensate and gas phase reactions [23], [24], [25]

The main reason for using epoxy is its excellent mechanical strength. Epoxy also has excellent resistance to chemicals [26], [27]. Epoxy resin has a lower pyrolysis ratio and better thermal stability ([28], [29]). In this research, variations in the addition of epoxy were carried out in the manufacture of solid propellant. The dependence of the propellant burning rate on the initial pressure and temperature is one of the most important characteristics from the point of view of its application in weapons systems [30], [31], [32].

In this research, the solid propellant used was a mixture of AP, epoxy and aluminum powder. The composition of the materials used can be seen in Table 1. The resulting solid propellant was printed with a length of 10 cm. The test results obtained are data on the propellant burning time as shown in Table 2. Based on the test results, the propellant burning rate will be calculated using the formula in Equation 1. The graphic results of the burning speed against the propellant burning time are shown in Figure 2.

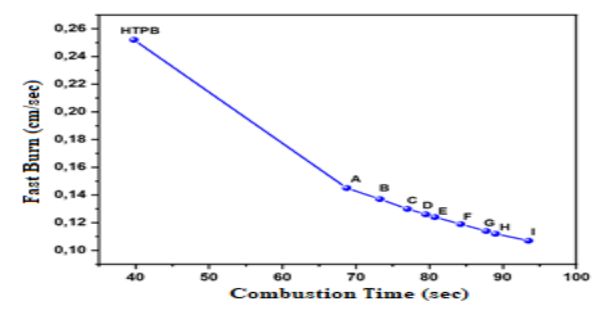


Figure 2. Graphic results of burning speed versus propellant combustion time with variations in composition.

Figure 2 shows that the increasing number of epoxy variations causes the burning time to become longer so that the propellant burns faster. The burn rate produced using HTPB is higher than using epoxy. The highest burn rate using epoxy is composition A. The higher the epoxy, the lower the burn rate produced. The resulting combustion temperature results are shown in Table 3.

Based on the results of the combustion temperature, the specific heat ratio will be known by carrying out calculations using the formula in Equation 2. The graph of the calculation results of the specific heat ratio to propellant combustion temperature with variations in composition can be shown in Figure 3. It shows that the increasing addition of epoxy variations causes the combustion temperature to increase, causing the specific heat ratio to decrease. The highest combustion temperature is found in the HTPB composition. The highest burning temperature using epoxy is found in composition A.

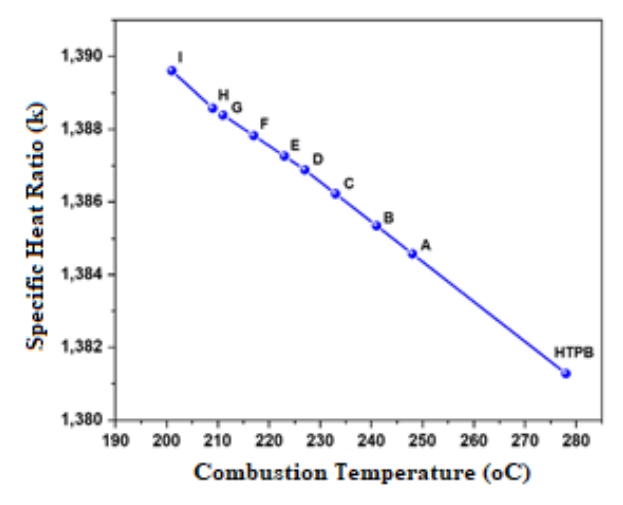


Figure 3. Graphic results of the ratio of specific heat to propellant combustion temperature with variations in composition.

The higher the epoxy temperature, the lower the combustion produced. The results of the combustion temperature are inversely proportional to the specific heat ratio. The higher the combustion temperature, the lower the specific ratio produced. The results of the combustion temperature affect the temperature in the chamber.

The results of the chamber temperature calculation can be seen in Table 3. The results of the chamber temperature graph against combustion temperature are in Figure 4.

Figure 4 shows that the increasing addition of epoxy variations causes the combustion temperature and chamber temperature to increase. The highest chamber temperature is found in the HTPB composition. The highest chamber temperature using epoxy is found in composition A. The less epoxy added, the higher the resulting chamber temperature. The resulting chamber temperature will affect the chamber pressure.

The results of the pressure in the chamber can be seen in Table 5. The results of the graph of chamber pressure against chamber temperature with variations in composition can be seen in Figure 5.

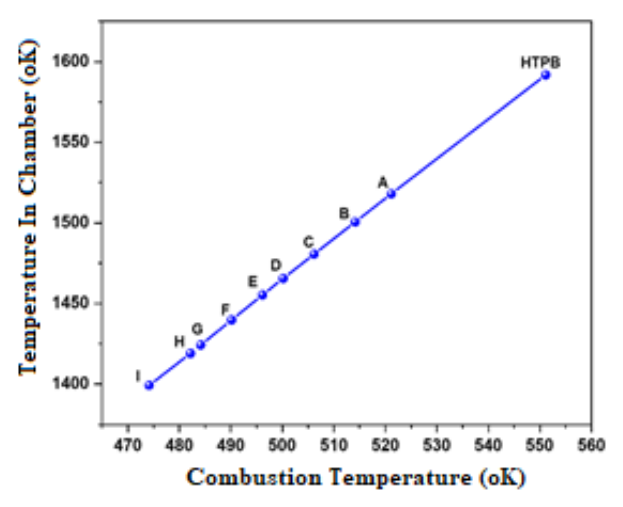


Figure 4. Graphic results of temperature in the chamber against combustion temperature with variations in composition.

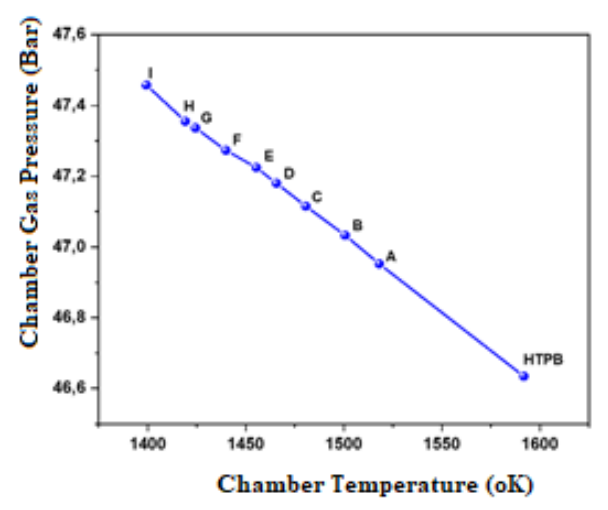


Figure 5. Graphic results of chamber gas pressure against chamber temperature with variations in composition.

Figure 5 shows that as the chamber temperature increases, the resulting chamber gas pressure decreases. The highest gas pressure in the chamber is in composition I. The increasing addition of epoxy causes the gas pressure in the chamber to increase. The resulting pressure in the chamber will affect the resulting throat pressure.

The resulting throat pressure can be calculated using Equation 9. The results of the throat pressure calculation can be seen in Table 5. The graphical results of the gas pressure in the throat versus the gas pressure in the chamber with variations in composition are shown in Figure 6.

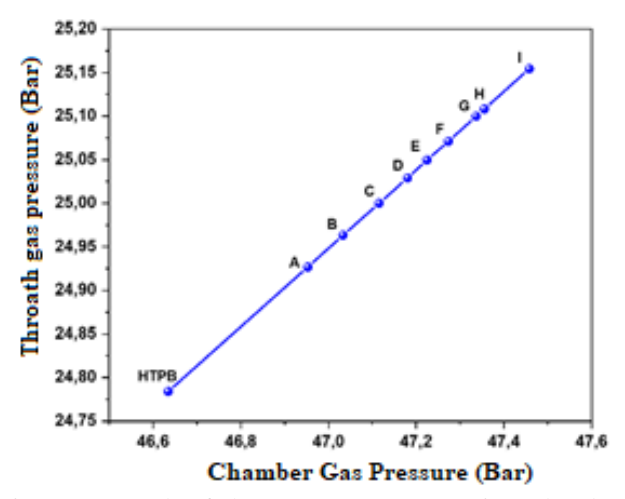


Figure 6. Graph of throat gas pressure against chamber temperature with variations in composition.

Figure 6 shows that the increasing number of epoxy variations causes the gas pressure in the throat and chamber to increase. thus causing the specific heat ratio to decrease. The highest gas pressure in the throat lies in composition I. So, as the addition of epoxy increases, the gas pressure in the throat increases.

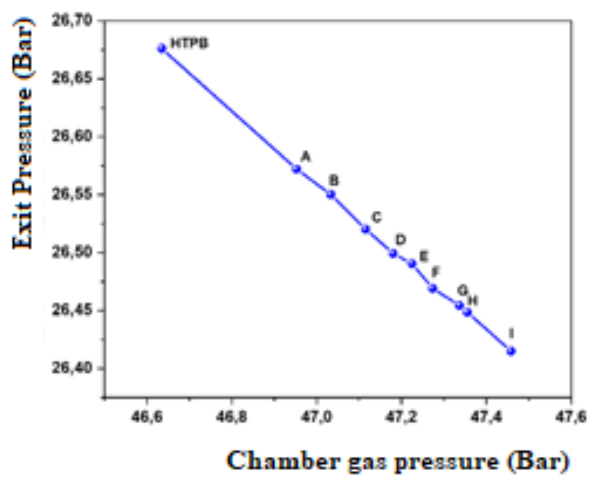


Figure 7. Graphical results of gas exit pressure against chamber temperature with variations in composition.

The pressure in the chamber will also affect the pressure at the resulting exit. Figure 7 shows that as the gas pressure in the chamber increases, the resulting exit pressure decreases. The highest exit pressure is found in the HTPB composition. The highest exit pressure using epoxy is in variation A. The increase in epoxy addition causes the resulting exit pressure to be lower. The results of the combustion gas velocity calculation can be seen in Table 5. The graphical results of the combustion gas velocity versus propellant combustion speed with variations in composition can be seen in Figure 8.

Figure 8 shows that as the combustion speed increases, the velocity of the propellant combustion gas increases. The highest combustion gas velocity is found in composition variations using HTPB. The highest combustion gas velocity using epoxy is found in variation A. The increasing addition of epoxy results in the lower combustion gas

velocity produced. The speed of the combustion gas will affect the mass flow rate results.

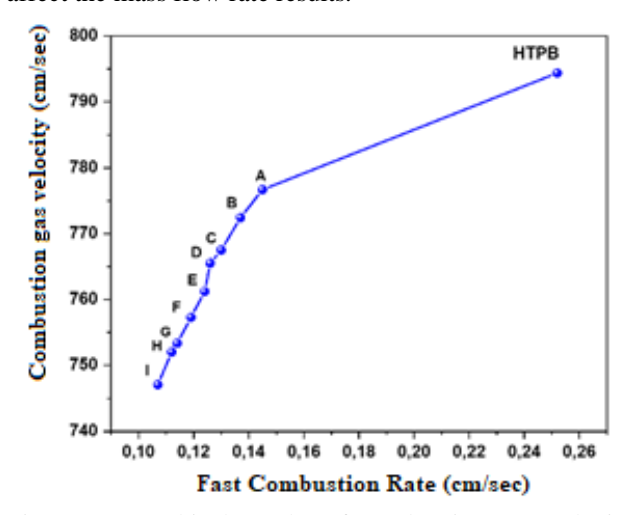


Figure 8. Graphical results of combustion gas velocity versus propellant combustion speed with variations in composition

The graphical results of the gas mass flow rate against propellant combustion speed with variations in composition can be seen in Figure 9.

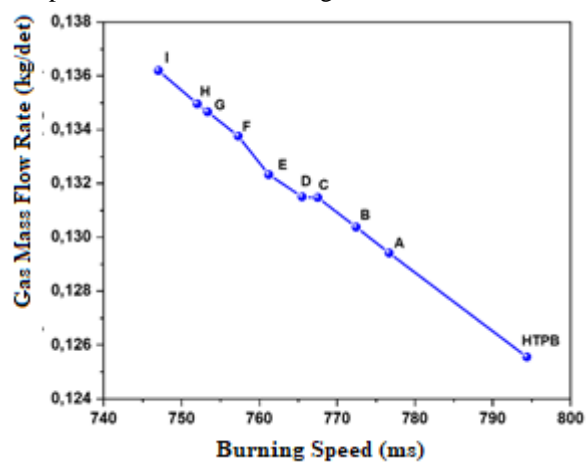


Figure 9. Graphical results of gas mass flow rate against propellant combustion speed with variations in composition.

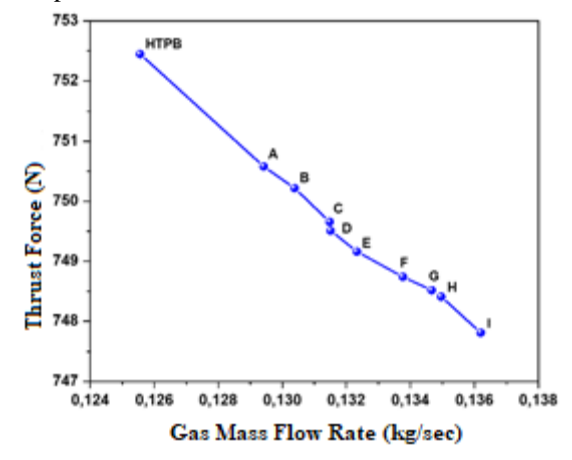


Figure 10. Graph of thrust force against gas mass flow rate with variations in composition.

Evrimata: Journal of Mechanical Engineering Vol. 01, No. 03, June, 2024, p.69 – 76

Figure 9 shows that as the gas combustion speed increases, the mass flow rate of the resulting gas decreases. The highest gas mass flow rate results are in composition I. The increasing addition of epoxy causes the gas mass flow rate to increase. Based on the gas mass flow rate, exit pressure, combustion gas velocity will affect the resulting thrust force. The results of the thrust force calculation can be seen in Table 5.

Figure 10 shows that as the gas mass flow rate increases, the resulting thrust force decreases. The highest thrust force results were found in the HTPB composition of 752.4502 N. The highest thrust force results using epoxy were found in composition A formulation of 750.5771 N.

When a rocket is operating, its movement is caused by the thrust force that occurs from the propellant combustion reaction [33], [34]The greater the thrust, the greater the rocket's performance. The increasing addition of epoxy causes the resulting thrust force to decrease. The difference in maximum thrust force between HTPB and composition A is 1.8731 N. This shows that the performance of using epoxy is almost close to that of HTPB. The best composition formulation is composition A using 46% Ammonium Perchlorate, 36% Aluminum and 18% Epoxy.

CONCLUSION

The increase in the addition of epoxy results in a decrease in the fuel propagation speed, combustion temperature, exit pressure, combustion gas speed so that the resulting thrust force decreases. The most optimum composition in this research was composition A using 46% Ammonium Perchlorate, 36% Aluminum and 18% Epoxy. The difference in pushing force between HTPB and composition A is 1.8731 N. This proves that epoxy can be used as a substitute for HTPB.

6. ACKNOWLEDGEMENTS

The authors would like to thank Army Polytechnic of Malang, Indonesia for the experimental supports.

7. AUTHOR CONTRIBUTIONS

Conception and design: Maryono, Muhammad.Ali Methodology: Lazuardi

Data acquisition: Muhammad.Ali

Analysis and interpretation of data: Maryono,

Writing publication: Muhammad.Ali, Lazuardi

Approval of final publication: Maryono, Muhammad.Ali, Resources, technical and material supports: Maryono,

Supervision: Lazuardi

8. REFERENCES

- [1] F. Piscitelli, G. Saccone, A. Gianvito, G. Cosentino, and L. Mazzola, "Characterization and manufacturing of a paraffin wax as fuel for hybrid rockets," Propuls. Power Res., vol. 7, no. 3, pp. 218–230, 2018, doi: 10.1016/j.jppr.2018.07.007.
- [2] E. T. Sandall, J. Kalman, J. N. Quigley, S. Munro, and T. D. Hedman, "A study of solid ramjet fuel containing boron–magnesium mixtures," Propuls. Power Res., vol. 6, no. 4, pp. 243–252, 2017, doi: 10.1016/j.jppr.2017.11.004.
- [3] D. Zhang et al., "Using microfluidic technology to prepare octogen high-energy microspheres containing copper–aluminum composite particles with enhanced combustion performance," Mater. Des., vol. 229, p. 111874, 2023, doi: 10.1016/j.matdes.2023.111874.

- [4] H. Li, J. Wei, Y. nan Zhang, Y. bing Hu, W. Jiang, and T. yue Zhang, "GO/HTPB composite liner for anti-migration of small molecules," Def. Technol., vol. 22, pp. 156–165, 2023, doi: 10.1016/j.dt.2021.11.006.
- [5] F. yao Chen et al., "A review on the high energy oxidizer ammonium dinitramide: Its synthesis, thermal decomposition, hygroscopicity, and application in energetic materials," Def. Technol., vol. 19, pp. 163–195, 2023, doi: 10.1016/j.dt.2022.04.006.
- [6] C. Wang et al., "Micro-aluminum powder with bi- or tri-component alloy coating as a promising catalyst: Boosting pyrolysis and combustion of ammonium perchlorate," Def. Technol., vol. 33, pp. 100–113, 2024, doi: 10.1016/j.dt.2023.06.001.
- [7] P. Zhang, L. Sun, J. Yuan, and J. Deng, "Synthesis of multifunctional additives for solid propellants: Structure, properties and mechanism," Def. Technol., vol. 33, pp. 308–316, 2024, doi: 10.1016/j.dt.2023.06.009.
- [8] Y. Zhang, N. Wang, W. Ma, R. Wang, L. Bai, and Y. Wu, "Investigations of the mechanical response of dummy HTPB propellant grain under ultrahigh acceleration overload conditions using onboard flight-test measurements," Def. Technol., vol. 32, pp. 473–484, 2024, doi: 10.1016/j.dt.2023.04.003.
- [9] L. Dong, Y. Wu, K. Yang, and X. Hou, "Investigation of high rate mechanical flow followed by ignition for high-energy propellant under dynamic extrusion loading," Def. Technol., vol. 32, pp. 336– 347, 2024, doi: 10.1016/j.dt.2023.05.009.
- [10]H. Yang et al., "A review on surface coating strategies for antihygroscopic of high energy oxidizer ammonium dinitramide," Def. Technol., vol. 33, pp. 237–269, 2024, doi: 10.1016/j.dt.2023.08.012.
- [11] T. Kovačević, S. Mijatov, J. Gržetić, S. Cakić, B. Fidanovski, and S. Brzić, "The effect of reactive plasticizer on viscoelastic and mechanical properties of solid rocket propellants based on different types of HTPB resin," Def. Technol., vol. 33, pp. 66–77, 2024, doi: 10.1016/j.dt.2023.11.020.
- [12] A. Debnath, Y. Pal, S. N. Mahottamananda, and D. Trache, "Unraveling the role of dual Ti/Mg metals on the ignition and combustion behavior of HTPB-boron-based fuel," Def. Technol., vol. 32, pp. 134–143, 2024, doi: 10.1016/j.dt.2023.07.005.
- [13] W. Zhou, M. Zhao, B. Liu, Y. Ma, Y. Zhang, and X. Wang, "Investigation of hydroxyl-terminated polybutadiene propellant breaking characteristics and mechanism impacted by submerged cavitation water jet," Def. Technol., vol. 33, pp. 559–572, 2024, doi: 10.1016/j.dt.2023.08.011.
- [14]S. Jain, G. Gupta, D. R. Kshirsagar, V. H. Khire, and B. Kandasubramanian, "Burning rate and other characteristics of strontium titanate (SrTiO3) supplemented AP/HTPB/Al composite propellants," Def. Technol., vol. 15, no. 3, pp. 313–318, 2019, doi: 10.1016/j.dt.2018.10.004.
- [15]P. Kumar, "Advances in phase stabilization techniques of AN using KDN and other chemical compounds for preparing green oxidizers," Def. Technol., vol. 15, no. 6, pp. 949–957, 2019, doi: 10.1016/j.dt.2019.03.002.
- [16]Z. jun Wang, H. fu Qiang, G. Wang, and B. Geng, "Strength criterion of composite solid propellants under dynamic loading," Def. Technol., vol. 14, no. 5, pp. 457–462, 2018, doi: 10.1016/j.dt.2018.06.016.
- [17]L. ke Zhang and X. yang Zheng, "Experimental study on thermal decomposition kinetics of natural ageing AP/HTPB base bleed composite propellant," Def. Technol., vol. 14, no. 5, pp. 422–425, 2018, doi: 10.1016/j.dt.2018.04.007.
- [18] K. Ghosh et al., "Light weight HTPB-clay nanocomposites (HCN) with enhanced ablation performance as inhibition materials for composite propellant," Def. Technol., vol. 17, no. 2, pp. 559–570, 2021, doi: 10.1016/j.dt.2020.03.011.
- [19]Z. jun Wang and H. fu Qiang, "Mechanical properties of thermal aged HTPB composite solid propellant under confining pressure," Def. Technol., vol. 18, no. 4, pp. 618–625, 2022, doi: 10.1016/j.dt.2021.06.014.
- [20] N. bai He et al., "Burning surface formation mechanism of laser-controlled 5-aminotetrazole propellant," Def. Technol., vol. 25, pp. 48–59, 2023, doi: 10.1016/j.dt.2022.05.005.
- [21] A. Giri, V. K. Bharti, P. Garai, and K. P. Singh, "Ecotoxicology of magnesium-based explosive: impact on animal and human food chain," Discov. Sustain., vol. 4, no. 1, 2023, doi: 10.1007/s43621-023-00173-3.

- [22] D. Meng, L. Sang, P. Zhang, J. Deng, and X. Guo, "Properties of high cis-1,4 content hydroxyl-terminated polybutadiene and its application in composite solid propellants," Def. Technol., no. xxxx, pp. 1–11, 2024, doi: 10.1016/j.dt.2024.04.014.
- [23] M. Kohga, R. Togashi, H. Tsutiya, and Y. Ota, "Catalytic effect of ferric oxide on burning characteristics of propellants using ammonium perchlorate with varied particle properties," Combust. Flame, vol. 246, p. 112459, 2022, doi: 10.1016/j.combustflame.2022.112459.
- [24]R. Minato, "Low toxic nitromethane based monopropellant for gas generator cycle air turbo ramjet engine," Propuls. Power Res., vol. 11, no. 3, pp. 311–324, 2022, doi: 10.1016/j.jppr.2022.08.001.
- [25]R. Wang, N. Wang, J. Gao, Y. Zhang, A. Zhang, and Y. Wu, "Friction-induced ignition study of HTPB propellant based on a coupled chemo-mechano-thermodynamic model under ultrahigh acceleration overload conditions," Case Stud. Therm. Eng., vol. 52, no. October, 2023, doi: 10.1016/j.csite.2023.103708.
- [26] Q. NIU, Z. HE, and S. DONG, "IR radiation characteristics of rocket exhaust plumes under varying motor operating conditions," Chinese J. Aeronaut., vol. 30, no. 3, pp. 1101–1114, 2017, doi: 10.1016/j.cja.2017.04.003.
- [27] W. M. ADEL and G. LIANG, "Service life prediction of AP/Al/HTPB solid rocket propellant with consideration of softening aging behavior," Chinese J. Aeronaut., vol. 32, no. 2, pp. 361–368, 2019, doi: 10.1016/j.cja.2018.08.003.
- [28] H. Zhu, H. Tian, and G. Cai, "Hybrid uncertainty-based design optimization and its application to hybrid rocket motors for manned lunar landing," Chinese J. Aeronaut., vol. 30, no. 2, pp. 719–725, 2017, doi: 10.1016/j.cja.2017.02.009.
- [29] J. Chen, D. Meng, J. Deng, and P. Zhang, "Synthesis of unsaturated polyurethane oligomer and its application in the 3D printing of composite solid propellants," Mater. Des., vol. 238, no. January, p. 112675, 2024, doi: 10.1016/j.matdes.2024.112675.
- [30]P. Kumar, P. Chandra Joshi, R. Kumar, and S. Biswas, "Catalytic effects of Cu-Co* on the thermal decomposition of AN and AN/KDN based green oxidizer and propellant samples," Def. Technol., vol. 14, no. 3, pp. 250–260, 2018, doi: 10.1016/j.dt.2018.03.002.
- [31]P. Kumar, "An overview on properties, thermal decomposition, and combustion behavior of ADN and ADN based solid propellants," Def. Technol., vol. 14, no. 6, pp. 661–673, 2018, doi: 10.1016/j.dt.2018.03.009.
- [32] Y. bin LI, L. ping PAN, Z. jian YANG, F. yan GONG, X. ZHENG, and G. song HE, "The effect of wax coating, aluminum and ammonium perchlorate on impact sensitivity of HMX," Def. Technol., vol. 13, no. 6, pp. 422–427, 2017, doi: 10.1016/j.dt.2017.05.022.
- [33] Y. Hou, J. Xu, C. Zhou, and X. Chen, "Microstructural simulations of debonding, nucleation, and crack propagation in an HMX-MDB propellant," Mater. Des., vol. 207, p. 109854, 2021, doi: 10.1016/j.matdes.2021.109854.
- [34] R. Liu, D. Yang, K. Xiong, Y. L. Wang, and Q. L. Yan, "Fabrication and characterization of multi-scale coated boron powders with improved combustion performance: A brief review," Def. Technol., vol. 31, pp. 27–40, 2024, doi: 10.1016/j.dt.2023.03.015.